ARTICLE IN PRESS

Kafkas Universitesi Veteriner Fakultesi Dergisi
Journal Home-Page: http://vetdergikafkas.org
E-ISSN: 1309-2251

Kafkas Univ Vet Fak Derg
xx (x): xx-xx, 2024
DOI: 10.9775/kvfd.2024.32344

RESEARCH ARTICLE

Mitochondrial Fusion Protein 2 Affects Intracellular Survival of *Brucella abortus* A19 by Regulating Endoplasmic Reticulum Stress and Apoptosis

Zhenyu XU[1] Qin YANG[1] Xiaoyu DENG[1,2] Yimei XU[3] Zhongchen MA[1(*)] Chuangfu CHEN[1(*)]

[1] School of Animal Science and Technology, Shihezi University, 832000 Shihezi, Xinjiang, CHINA
[2]School of Basic Medicine, Hunan University of Medicine, 418000 huaihua, Hunan, CHINA
[3]Xinjiang Uygur Autonomous Region Center for Disease Control and Prevention, 830002 Urumq, Xinjiang, CHINA

(*) **Corresponding authors:** Chuangfu CHEN & Zhongchen MA

Phone: +86-13999328996 (C.C.), +86-18899596400 (ZM)
E-mail: ccf-xb@163.com (C.C.), zhongchen_ma@163.com (Z.M.)

How to cite this article?

Xu Z, Yang Q, Deng X, Xu Y, Ma Z, Chen C: Mitochondrial fusion protein 2 affects intracellular survival of Brucella abortus A19 by regulating endoplasmic reticulum stress and apoptosis. *Kafkas Univ Vet Fak Derg*, 2024 (Article in Press).
DOI: 10.9775/kvfd.2024.32344

Article ID: KVFD-2024-32344
Received: 21.05.2024
Accepted: 22.07.2024
Published Online: 16.08.2024

Abstract

Mitochondrial fusion protein 2 (MFN2) deficiency has been shown to hinder the survival of bacteria in macrophages. Endoplasmic reticulum stress and apoptosis are vital defense mechanisms against Brucella infection, but the specific role of MFN2 in Brucella-infected macrophages remains unclear. In this study, we aimed to investigate the role of MFN2 in the infection of macrophages by Brucella abortus strain A19. The levels of CHOP and GRP78, which are molecules associated with endoplasmic reticulum stress, as well as Caspase-3 and BAX, which are pro-apoptotic molecules, were measured using confocal microscopy, qRT-PCR and Western blot in cell models infected with B. abortus A19. Additionally, the apoptosis rate of these cell models was assessed using flow cytometry. Our findings revealed a significant decrease in MFN2 levels 24 h post B. abortus A19 infection of macrophages. Interfering with MFN2 in macrophages led to an increase in Brucella-induced up-regulation of CHOP, GRP78, Caspase-3, and BAX, consequently hindering the survival of B. abortus A19 in macrophages. Conversely, infecting macrophages that overexpress MFN2 with B. abortus A19 resulted in the down-regulation of CHOP, GRP78, Caspase-3, and BAX. MFN2 mediated the down-regulation of endoplasmic reticulum stress and programmed cell death in B. abortus A19-infected macrophages, thereby supported the intracellular survival of Brucella. This is the first report to highlight the key role of MFN2 in the intracellular survival of Brucella, providing a new perspective for understanding the mechanisms involved and offering a potential research direction for the development of targeted therapeutic agents against brucellosis.

Keywords: *Brucella abortus* A19, Mitochondrial fusion protein 2, Endoplasmic reticulum stress, Apoptosis, Intracellular survival

Introduction

Brucellosis is a zoonotic disease caused by *Brucella* species. It is a significant animal-borne disease that is widespread in over 170 countries and regions worldwide. In livestock, it commonly presents as a reproductive disorder, while in humans, it manifests as a chronic febrile illness. Due to its persistent nature and widespread prevalence, the disease is challenging to eliminate and poses a significant threat to both animal husbandry and human health [1-3].

The endoplasmic reticulum (ER) is a crucial organelle that plays a role in maintaining cellular homeostasis [4]. It synthesizes intracellular proteins and lipids and has close interactions with mitochondria, allowing for signaling and substance exchange. Mitochondrial fusion protein 2 (MFN2) is a GTPase protein found in the outer mitochondrial membrane and the mitochondria-associated membrane. It acts as a bridge between mitochondria and the endoplasmic reticulum, and its absence leads to endoplasmic reticulum stress. MFN2 also regulates mitochondrial fusion and the transfer of calcium from the endoplasmic reticulum to mitochondria [5]. Numerous studies have demonstrated the crucial role of MFN2 in the innate immune response during pathogenic infections [6-8]. Previous studies have shown that MFN2 inhibits the antiviral immune response in hepatitis B virus-associated hepatocellular carcinoma

[6]. In HIV-1 Vpr-infected HEK293 cells, overexpression of MFN2 reduces cell death by facilitating interactions between the endoplasmic reticulum and mitochondria [7]. Additionally, in *Mycobacterium tuberculosis*-infected THP-1 macrophages, MFN2 is involved in the assembly and activation of NLRP3 inflammatory vesicles during infection [8].

Brucella, an intracellular parasitic bacterium, employs various strategies to invade host cells. It primarily targets specialized phagocytes like macrophages, dendritic cells, as well as non-specialized phagocytes such as fibroblasts and trophoblasts. Once inside the host cells, *Brucella* releases effector molecules into the host cytoplasm. This facilitates *Brucella*'s transport to the endoplasmic reticulum (ER), resulting in significant reorganization of the ER and disruption of its homeostasis. These events induce ER stress, triggering the unfolded protein response (UPR), which aids in the survival and establishment of proliferative compartments [9,10]. In the context of ER stress, the transcription factor CHOP plays a crucial role. If the ER stress persists and overwhelms the capacity of the cellular response, it leads to increased expression of CHOP. In turn, CHOP acts as a major pro-apoptotic transcription factor, ultimately driving the cells towards apoptosis [11,12]. Glucose-regulated protein (GRP78) is a key chaperone protein located in the endoplasmic reticulum (ER). It is synthesized in response to various stress conditions that disrupt ER function and homeostasis [13]. *Brucella* has been shown to regulate apoptosis [14,15]. Inhibition of apoptosis in infected cells supports the intracellular replication of *Brucella* [15], with mitochondrial division being a crucial step in the apoptotic process. The pro-apoptotic protein BAX, a member of the Bcl-2 family, is recruited to the outer mitochondrial membrane during apoptosis, leading to mitochondrial fragmentation and blocking of mitochondrial fusion [16]. BAX, which is normally distributed in cytoplasmic lysates, plays a role in regulating mitochondrial morphology [17]. *Brucella* has been found to interact with mitochondria in host cells, a process that is essential for intracellular recycling and infection of neighboring cells by *Brucella* [10]. Caspase-3 is also an important marker of apoptosis. *Brucella* infection of RAW264.7 cells for 48 h can induce apoptosis by upregulating the expression of caspase-3 via the effector protein BtpB [15].

The role of MFN2 in *Brucella* infected host cells has not been investigated. To investigate the role of MFN2 during Brucella infection of cells, MFN2 was found to mediate the down-regulation of endoplasmic reticulum stress and programmed death in *B. abortus* A19-infected macrophages and to support the intracellular survival of *B. abortus* A19. Our study provides a theoretical basis for further investigation of the MFN2 gene and the pathogenesis of *Brucella*. In addition, the MFN2 gene may be a potential target for the future development of brucellosis prevention and therapeutic approaches.

Materials and Methods

Bacterial Strain and Cell Line

B. abortus A19 was purchased from the Xinjiang Tiankang Animal Biotechnology Co. Ltd., China. *B. abortus* was cultured on Tryptic Soy Agar (TSA) or Tryptic Soy Broth (TSB) (Oxoid, UK). The culture conditions in TSB were aerobic conditions at 37°C, 170 r/min for 3-4 d. *Escherichia coli* strains DH5α and BL21 were used to transform the PCDNA3.1-EGFP-MFN2 overexpression recombinant plasmid and were cultured on Luria-Bertani (LB) medium (Oxoid, UK) under aerobic conditions at 37°C and 170 r/min for 12 h. The mouse macrophage RAW264.7 line (RAW264.7, TIB-71) cell line (obtained from Cell Resource Center, IBMS, CAMS/PUMC, Beijing, China) was cultured in Dulbecco's modified Eagle's medium (DMEM, Gibco, USA) supplemented with 10% fetal bovine serum (FBS, Gibco, USA) at 37°C with 5% CO_2. All research work on *B. abortus* A19 was conducted in a biosafety level 3 laboratory.

Construction of MFN2 Interference and Overexpression Cell Models

The mRNA sequences of CHOP, GRP78, Caspase-3, BAX, MFN2 and GAPDH genes of mice published on the NCBI website GenBank were retrieved and primers were designed using Primer 5.0 *(Table1)*. The siRNA interference fragments (siMFN2-2275, siMFN2-450, siMFN2-1661) were synthesized by Anhui General Biological Company (Anhui, China) *(Table 2)*. The PCDNA3.1-EGFP plasmid (Anhui General Bio, China) was digested by Hind III and BamH I and ligated with MFN2 gene to construct the PCDNA3.1-EGFP-MFN2 recombinant plasmid.

Table 1. *Primer sequence of qRT-PCR*

Gene	Primer Sequence (5'→3')
CHOP-F	5'-CTGGAAGCCTGGTATGAGGAT-3'
CHOP-R	5'-CAGGGTCAAGAGTAGTGAAGGT-3'
GRP78-F	5'-ACTTGGGGACCACCTATTCCT-3'
GRP78-R	5'-ATCGCCAATCAGACGCTCC-3'
Caspase-3-F	5'-GAGCTTGGAACGCGAAGAAA-3'
Caspase-3-R	5'-TTGCGAGCTGACATTCCAGT-3'
BAX-F	5'-TGAAGACAGGGGCCTTTTTG-3'
BAX-R	5'-AATTCGCCGGAGACACTCG-3'
MFN2-F	5'-CCAACTCCAAGTGTCCGCTC-3'
MFN2-R	5'-GTCCAGCTCCGTGGTAACATC-3'

Table.2. Interference sequence of MFN2 siRNA	
Name	**Sequence (5'→3')**
siMFN2-450-F	5'-ACACAUGGCUGAAGUGAAUTT-3'
siMFN2-450-R	5'-AUUCACUUCAGCCAUGUGUTT-3'
siMFN2-1661-F	5'-CGGAGGAAGUGGAAAGGCATT-3'
siMFN2-1661-R	5'-UGCCUUUCCACUUCCUCCGTT-3'
siMFN2-2275-F	5'-GCAGUGGGCUGGAGACUCATT-3'
siMFN2-2275-R	5'-UGAGUCUCCAGCCCACUGCTT-3'
siMFN2-Negative-F	5'-UUCUCCGAACGUGUCACGUTT-3'
siMFN2-Negative-R	5'-ACGUGACACGUUCGGAGAATT-3'

Interference and overexpression systems were constructed by transfecting murine macrophage RAW264.7 cells with interference fragments and recombinant plasmids using Advanced DNA RNA Transfection Reagent (Zeta Life, USA).

Detection of Interference Efficiency of siRNA on MFN2

RAW264.7 cells were transiently transfected with siMFN2-2275, siMFN2-450, siMFN2-1661, and siMFN2-Negative interfering sequences at concentrations of 10 nM/μL as described previously [18], and cellular RNA and total protein were collected 48 h after transfection. Subsequently, the RNA was reverse transcribed into cDNA followed by the use of qRT-PCR to detect the mRNA expression level of MFN2. Cellular proteins were collected and the MFN2 protein expression level was assessed using Western blot analysis.

Interference efficiency = (siRNA-negative control group - siRNA experimental group)/siRNA - negative control group × 100%

Detection of Overexpression Efficiency of PCDNA3.1-EGFP-MFN2 Recombinant Plasmid

The PCDNA3.1-EGFP-MFN2 recombinant plasmid at a concentration of 6 μg was transiently transfected into RAW264.7 cells as described previously [19], and RNA and total protein were collected from the cells at 48 h of transfection. Then, the RNA was reverse transcribed into cDNA, and the mRNA expression level of MFN2 gene was detected by qRT-PCR, and the protein expression level of MFN2 was detected by Western blot [19].

Detection of *B. abortus* A19-Induced CHOP, GRP78, Caspase-3, BAX Expression Levels After MFN2 Interference and Overexpression

Interfering cells and overexpressing cell models were infected with *B. abortus* A19 respectively, and cellular RNA and total protein were collected at 24 h post-infection. Expression levels of endoplasmic reticulum stress signature molecules CHOP and GRP78 were detected by confocal microscopy. qRT-PCR and Western blot were used to detect the mRNA transcript and protein expression levels of endoplasmic reticulum stress signature molecules CHOP, GRP78 and pro-apoptotic genes Caspase-3 and BAX.

Detection of Apoptosis Induced by *B. abortus* A19 After MFN2 Interference and Overexpression

B. abortus A19 was used to infect the MFN2-interfering cell model and overexpressing cell model, respectively. Cells were collected at 24 h post-infection, digested with EDTA-free trypsin, adjusted to a cell concentration of 1-5x10^5/mL, and centrifuged at 800 rpm for 5 min before discarding the supernatant, and the cells were washed twice using PBS, and then processed in accordance with the apoptosis assay kit (Absin, China), and then immediately detected by flow cytometry.

Intracellular Survival of *B. abortus* A19 After MFN2 Interference and Overexpression

The best interfering and overexpressing cell models were infected with *B. abortus* A19 respectively, and the cells were lysed with 0.02% Triton X-100 at 0, 6, 12, and 24 h post-infection, and the lysates were coated in *B. abortus* solid medium and assayed for intracellular survival of *Brucella* by CFU counting with reference to the experimental method of Zhang et al.[20].

Confocal Microscopy Inspection

After 24 h of infection with *B. abortus* A19 in interfering and overexpressing cell models, cells were fixed on coverslips using 4% paraformaldehyde for 15 min. Subsequently, coverslips were rinsed thrice with PBS, and cells were treated with 0.2% Triton X-100 for 5 min. After another round of rinsing with PBS, cells underwent blocking in a blocking solution for 1 h. The primary antibody was then diluted with PBST and incubated in a dark, humid environment for 1 h at 4°C. Samples were incubated overnight, followed by washing thrice with PBST. The secondary antibody was diluted with PBST and samples were incubated for 1 h at room temperature in a dark, humid environment. After another round of washing with PBST, samples were sealed on slides using a DAPI-containing sealing agent, and finally examined under a fluorescence microscope.

qRT-PCR Detection

After infection of the interfering and overexpressing cell models by *B. abortus* A19, total RNA from the cells was collected and reverse transcribed to cDNA, and GAPDH was used as an internal reference, using the SYBR Green Master Mix kit (Roche, Switzerland) on QuantStudio 3

(ThermoFisher, USA). Real-time fluorescent quantitative PCR was performed, and the 2-ΔΔCt method was used to calculate the relative expression of CHOP, GRP78, Caspase-3, BAX and MFN2 mRNAs.

Western Blot Detection

B. abortus A19 infected cells were washed 3 times with PBS, lysed on ice for 10 min by adding lysis solution (1mLRIPA+10 μLPMSF), the lysate was collected and total protein was collected by centrifugation at 4°C, 12000 rpm for 5 min, and the protein was adjusted by BCA protein quantitative assay kit (ThermoFisher, USA). The concentration of protein was adjusted by BCA protein quantification kit (ThermoFisher, USA), separated by 12% SDS-PAGE and transferred to nitrocellulose (NC) membrane, closed with closure solution (5% skimmed milk powder in TBST) for 2 h at 37°C, washed 3 times with PBS and incubated with primary antibody diluted with TBST overnight at 4°C, washed 3 times with TBST and incubated with secondary antibody diluted with TBST at room temperature for 2 h. The membrane was washed with TBST 3 times and then stained with an ECL kit (ThermoFisher, USA).

Statistical Analysis

Data on intracellular CFU of *Brucella* were transformed into logarithms. The experimental data were analysed by One-Way ANOVA and 2 way ANOVA using SPSS 25.0 software (International Business Machines Corporation, USA), and the results were expressed as mean ± standard deviation, with $P<0.05$ considered statistically significant. GraphPad Prism 7.0 software (GraphPad Software, USA) was used to plot the data. All experiments were independently performed at least three times.

Results

B. abortus A19 Infection Induces a Decrease in Macrophage MFN2 Expression

Cells were collected at 6 h, 12 h and 24 h after *B. abortus* infection and the expression level of MFN2 was analysed by qRT-PCR and Western blotting. The results showed that the mRNA transcript level ($P=0.0047$) and protein expression level ($P=0.028$) of MFN2 were significantly reduced 24 h after *B. abortus* A19 infection of RAW264.7 cells, indicating that *B. abortus* A19 induced a decrease in macrophage MFN2 expression over time *(Fig. 1)*.

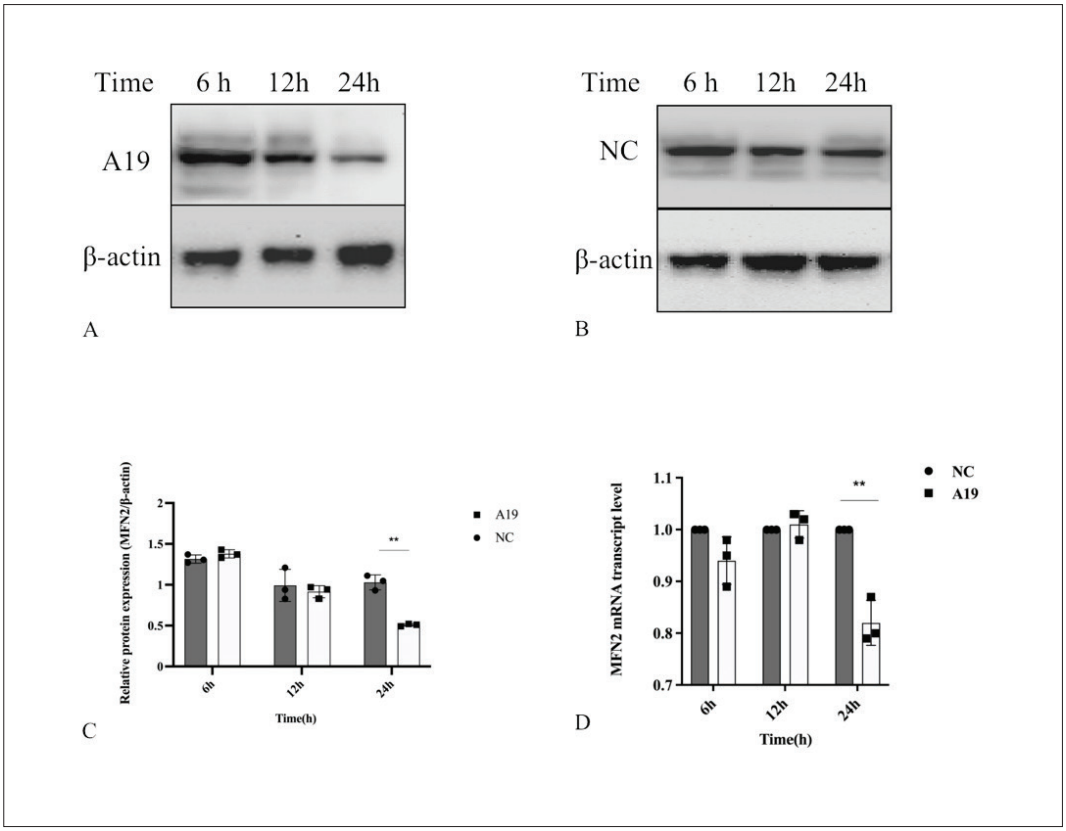

Fig 1. Detection of MFN2 mRNA and protein expression levels after *B. abortus* A19 infection. (A) Levels of MFN2 protein expression in RAW264.7 after infection with *B. abortus* A19 for 6, 12 and 24 h, (B) Negative control RAW264.7 cells MFN2 protein expression level after 6, 12 and 24 h (C), The ratio of cleaved MFN2 relative to β-actin levels was calculated using ImageJ. The experiment was repeated three times and data represent mean ± SD, (D) MFN2 mRNA expression levels were detected by qRT-PCR after 6 h, 12 h, and 24 h of *Brucella* abortus A19 infection in RAW264.7 cells. *$P<0.05$; **$P<0.01$

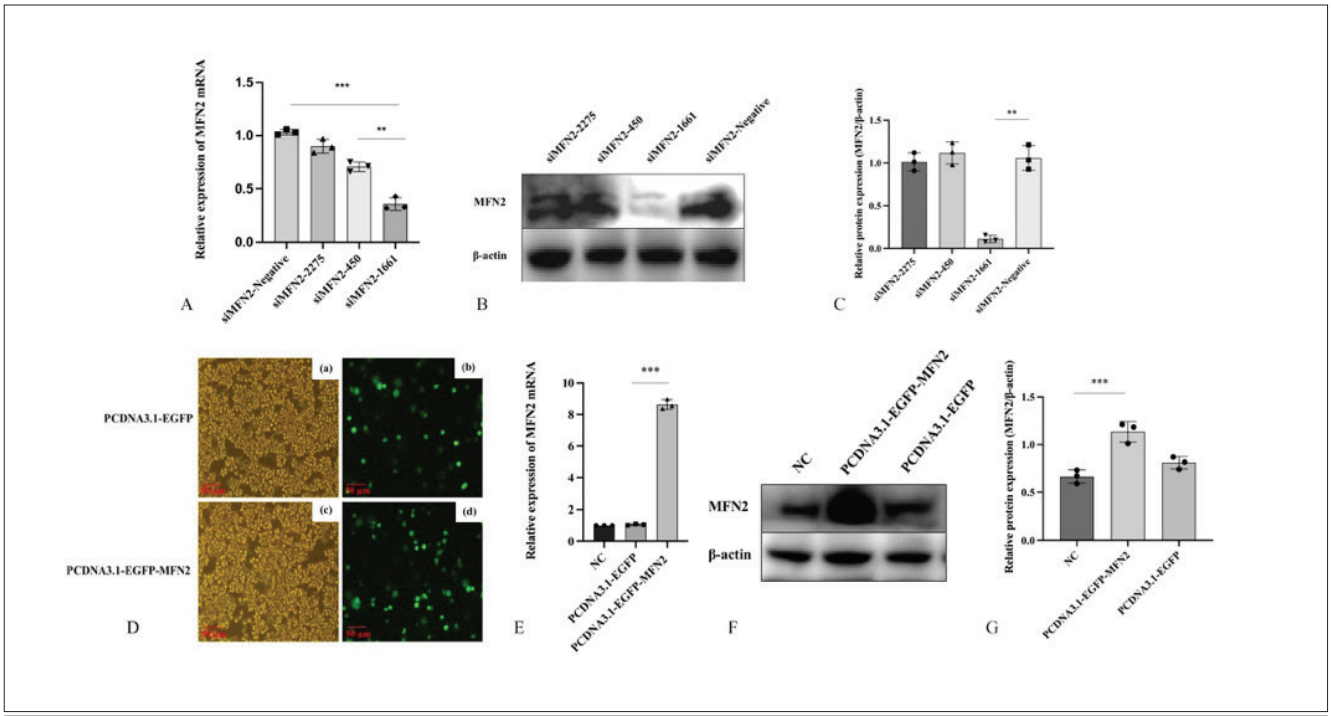

Fig 2. MFN2 overexpression and interference cell model construction. (A) qRT-PCR screening for the best interfering fragments of MFN2, (B) Western blot screening for the best interfering fragments of MFN2, (C) The ratio of cleaved MFN2 relative to β-actin levels was calculated using ImageJ. The experiment was repeated three times and data represent mean ± SD, (D) Transfection efficiency of PCDNA3.1-EGFP-MFN2 overexpression recombinant plasmid by fluorescence microscopy. (a, b: PCDNA3.1-EGFP transfection of RAW264.7 in bright and dark field view, b, c: PCDNA3.1-EGFP-MFN2transfection of RAW264.7 in bright and dark field view), (E) Efficiency of MFN2 gene overexpression detected by qRT-PCR, (F) Efficiency of MFN2 gene overexpression detected by Western blot, (G) The ratio of cleaved MFN2 relative to β-actin levels was calculated using ImageJ. The experiment was repeated three times and data represent mean ± SD. **P<0.01; ***P<0.001

Infection and Overexpression Cell Model Construction

The optimal interfering sequence was screened using qRT-PCR and Western blotting. The results showed that siMFN2-1661 had the highest inhibition rate (P<0.001) of MFN2 mRNA compared with the control group (siMFN2-Negative group) *(Fig. 2-A,B,C)*. This suggests that siMFN2-1661 is the best interfering fragment for constructing the MFN2 gene interference cell model.

After transfection of the recombinant plasmid PCDNA3.1-EGFP-MFN2 into RAW264.7 cells for 48h, a large amount of green fluorescent protein expression was observed by inverted fluorescence microscopy *(Fig. 2-D)*, indicating that the overexpression recombinant plasmid was successfully transfected. qRT-PCR results showed that compared with the control group (PCDNA3.1-EGFP group), the overexpression group (PCDNA3.1-EGFP-MFN2 group) had a significantly higher expression level of MFN2 mRNA than the control group, and the expression amount was about 8 times higher than that of the non-overexpressed group (PCDNA3.1-EGFP group) (P<0.001) *(Fig. 2-E)*. The Western blotting results showed that the expression level of MFN2 protein in the overexpression group was significantly higher than that in the control group (P<0.001) *(Fig. 2-F,G)*, indicating that the MFN2 gene overexpression cell model was successfully constructed.

B. abortus A19 Infection of MFN2 Deficient Macrophages Causes Up-Regulation of CHOP, GRP78, Caspase-3 and BAX

The interfering cell model was infiltrated with *B. abortus* A19, and the RNA and total protein of the infected cells were collected 24 h later. Results showed that the levels of mRNA transcript and protein expression of CHOP and GRP78, which are characteristic molecules of endoplasmic reticulum stress, in the interference group were significantly higher than those in the control group *(Fig. 3-A,B,C,D,G,H)*. The apoptotic molecules Cleaved caspase-3 and BAX mRNA transcript and protein expression levels were significantly higher in the interference group than in the control group *(Fig. 3-E,F,I,J)*. The results suggest that interference with the MFN2 gene enhances the ability of *B. abortus* A19 to induce endoplasmic reticulum stress and apoptosis.

B. abortus A19 Infection of Macrophages Overexpressing MFN2 Results in Down-Regulation of CHOP, GRP78, Caspase-3 and BAX

B. abortus A19 infection overexpression cell model, results showed that the endoplasmic reticulum stress signature molecules CHOP, GRP78 mRNA transcript level and protein expression level were significantly reduced in

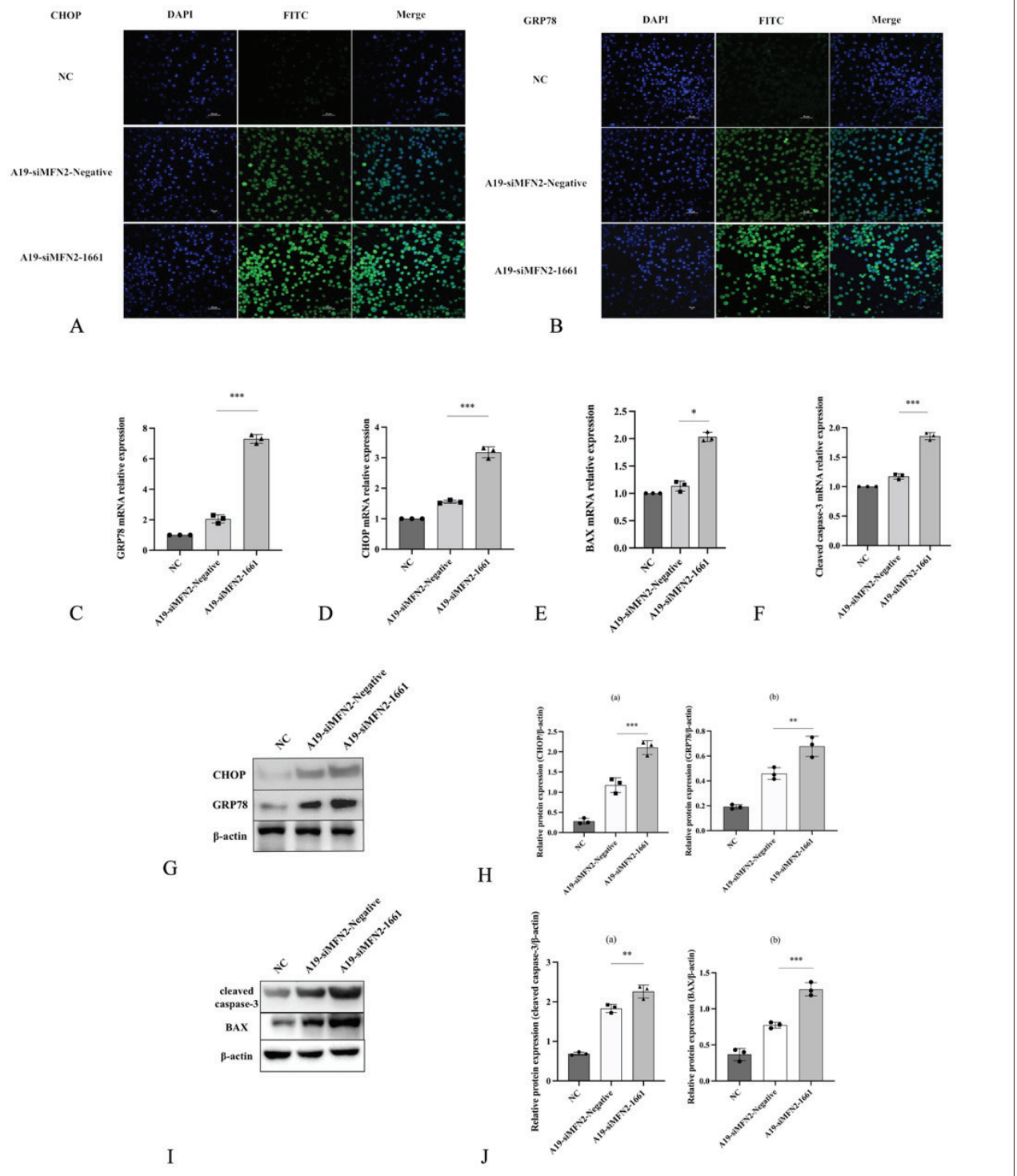

Fig 3. Expression levels of CHOP, GRP78, caspaes-3 and BAX were detected in the interfering cell model. (A) Confocal microscopy to detect CHOP spots 24 h after infection with the interfering cell model. CHOP spots are presented in green (FITC), while blue (DAPI) denotes nucleus, (B) Confocal microscopy to detect GRP78 spots 24 h after infection with the interfering cell model. GRP78 spots are presented in green (FITC), while blue (DAPI) denotes nucleus, (C)The expression level of GRP78 mRNA was detected by qRT-PCR after infection with *B. abortus* A19 in the interference cells model, (D) The expression level of CHOP mRNA was detected by qRT-PCR after infection with *B. abortus* A19 in the interference cells model, (E) The expression level of BAX mRNA was detected by qRT-PCR after infection with *B. abortus* A19 in the interference cells model, (F) The expression level of cleaved caspase-3 mRNA was detected by qRT-PCR after infection with *B. abortus* A19 in the interference cells model, (G) Expression levels of CHOP and GRP78 protein after infection with *B. abortus* A19 in the interference cells model, (H) The ratio of CHOP (a) and GRP78 (b) relative to β-actin levels was calculated using ImageJ. The experiment was repeated three times and data represent mean ± SD, (I) Expression levels of Cleaved caspase-3 and BAX protein after infection with *B. abortus* A19 in the interference cells model, (J) The ratio of cleaved caspase-3 (a) and BAX (b) relative to β-actin levels was calculated using ImageJ. The experiment was repeated three times and data represent mean ± SD. **P<0.05; **P<0.01; ***P<0.001*

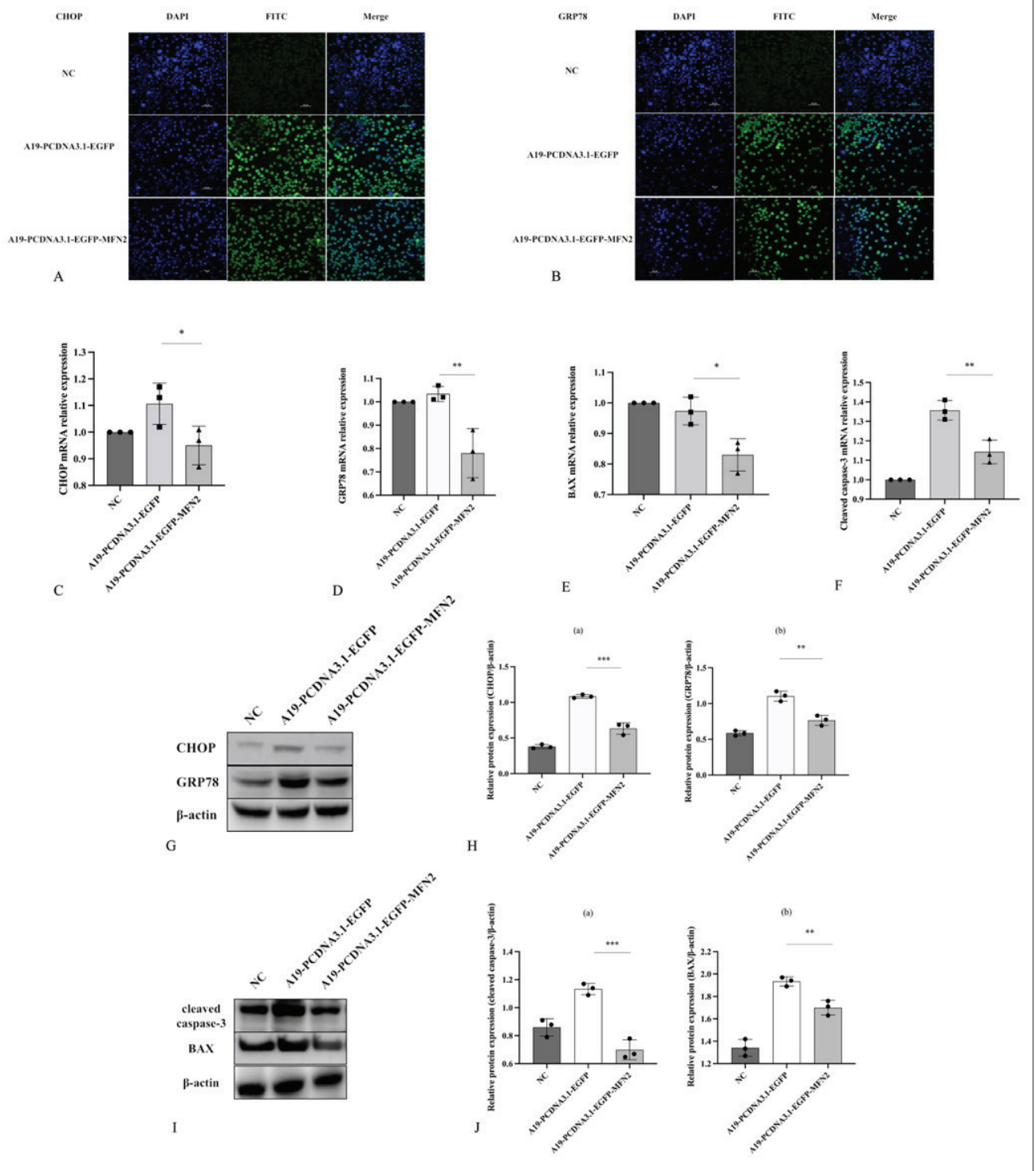

Fig 4. Expression levels of CHOP, GRP78, caspase-3 and BAX were detected in the overexpressing cell model. (A) Confocal microscopy to detect CHOP spots 24 h after infection with the overexpressing cell model. CHOP spots are presented in green (FITC), while blue (DAPI) denotes nucleus, (B) Confocal microscopy to detect GRP78 spots 24 h after infection with the overexpressing cell model, (C) The expression level of CHOP mRNA was detected by qRT-PCR after infection with *B. abortus* A19 in the overexpressing cell model, (D)The expression level of GRP78 mRNA was detected by qRT-PCR after infection with *B. abortus* A19 in the overexpressing cell model, (E) The expression level of BAX mRNA was detected by qRT-PCR after infection with *B. abortus* A19 in the overexpressing cell model, (F) The expression level of cleaved caspase-3 mRNA was detected by qRT-PCR after infection with *B. abortus* A19 in the overexpressing cell model, (G) Expression levels of CHOP and GRP78 protein after infection with *B. abortus* A19 in the overexpressing cell model, (H) The ratio of CHOP (a) and GRP78 (b) relative to β-actin levels was calculated using ImageJ. The experiment was repeated three times and data represent mean ± SD, (I) Expression levels of Cleaved caspase-3 and BAX protein after infection with *B. abortus* A19 in overexpressing cell model, (J) The ratio of cleaved caspase-3 (a) and BAX (b) relative to β-actin levels was calculated using ImageJ. The *experiment was repeated three times and data represent mean ± SD. *P<0.05; **P<0.01; ***P<0.001*

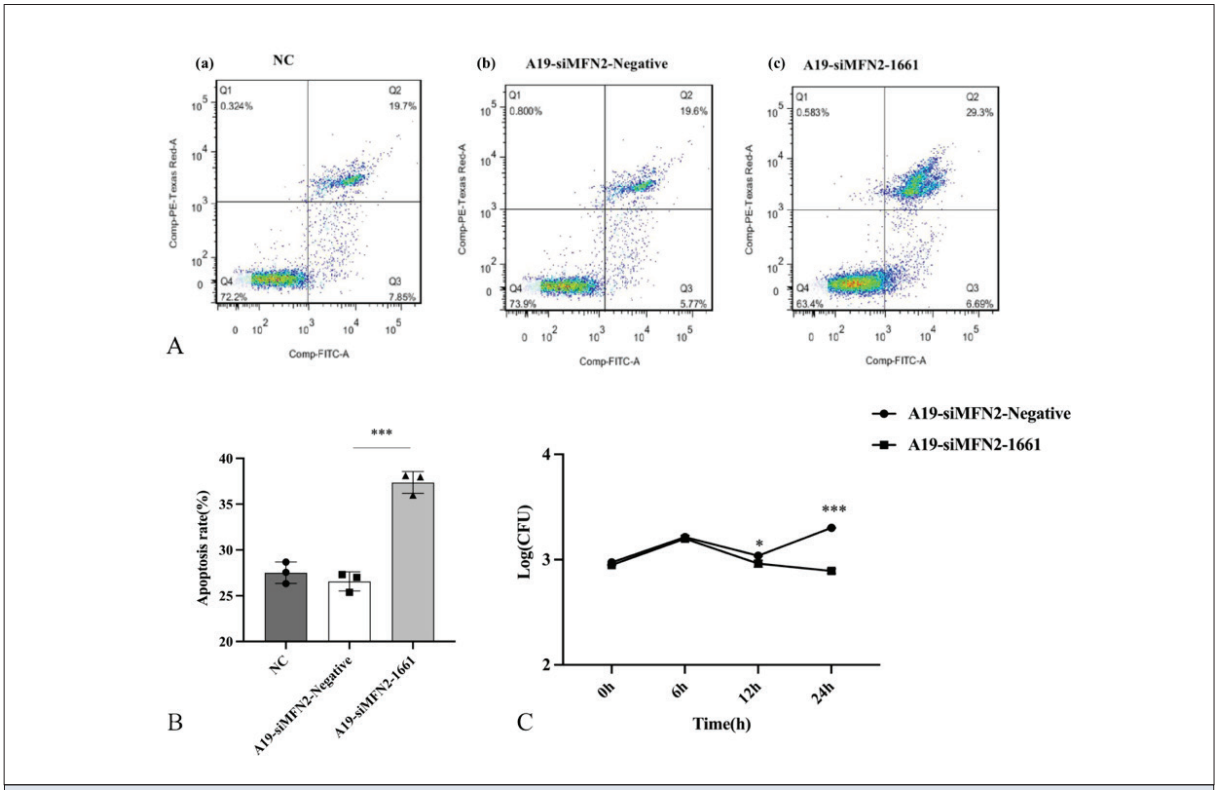

Fig 5. Apoptosis and *B. abortus* A19 intracellular survival in the *B. abortus* A19-induced interfering cell model. (A) Detection of apoptosis in *B. abortus* A19-induced interfering cell model cells by flow cytometry, (B) Bar graph of apoptosis rates in *B. abortus* A19-induced interfering cell models, (C) B. abortus A19 bacterial load in a model of interfering cells. ***P<0.001

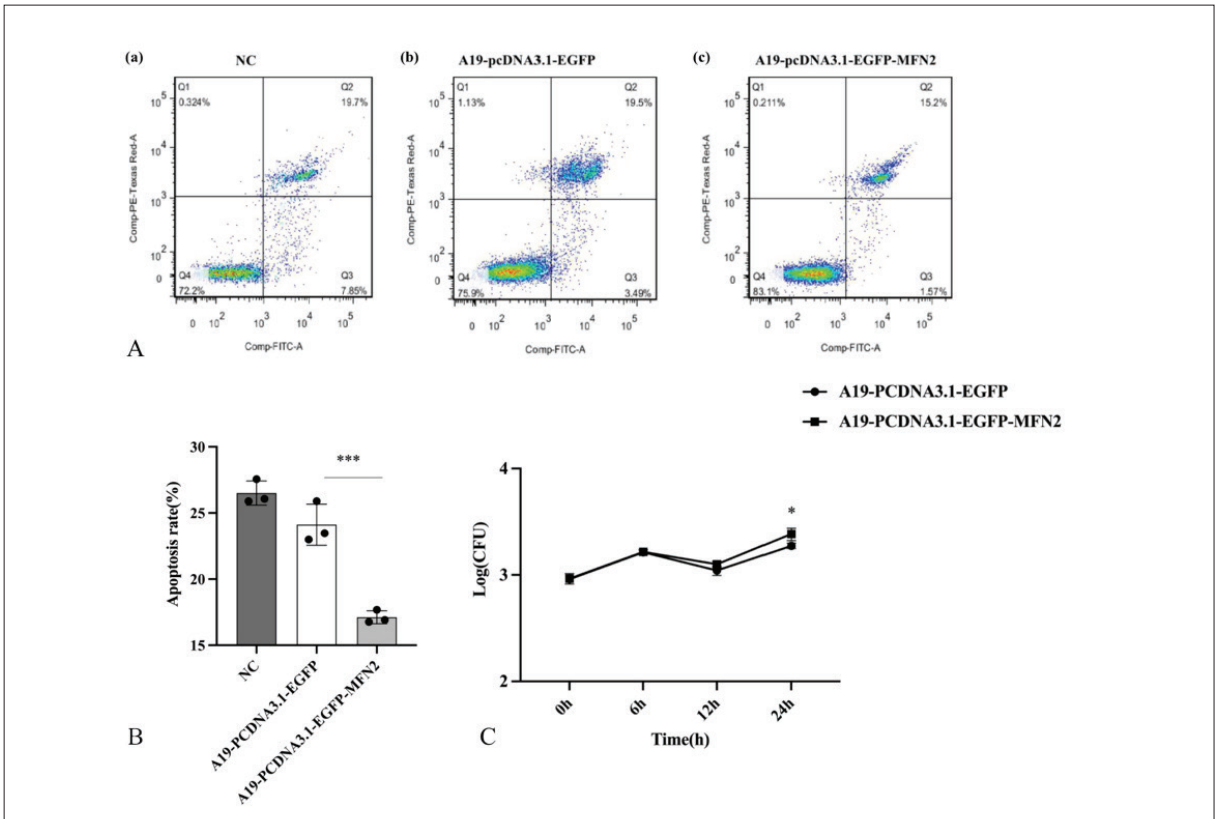

Fig 6. Apoptosis and *B. abortus* A19 intracellular survival in the *B. abortus* A19-induced overexpression cell model. (A) Detection of apoptosis in *B. abortus* A19-induced overexpression cell model by flow cytometry, (B) Bar graph of apoptosis rate in *B. abortus* A19-induced overexpressing cell models, (C) *B. abortus* A19 bacterial load in a model of overexpression cells. *P<0.05; ***P<0.001

the overexpression group compared with the control group *(Fig. 4-A,B,C,D,G,H)*, and the apoptosis signature molecules Cleaved caspase-3, BAX mRNA transcript and protein expression levels were also significantly reduced *(Fig. 4-E,F,H,J)*. This indicates that overexpression of MFN2 gene decreases the ability of *B. abortus* A19 to induce endoplasmic reticulum stress and apoptosis.

B. abortus A19 infection with Macrophages Lacking MFN2 Results in Decreased *B. abortus* A19 Intracellular Survival

B. abortus A19 infection was observed to have an impact on the MFN2 model cells. The cells were lysed at different time intervals and the number of viable bacteria inside the cells was measured. The results showed a significant decrease in the number of intracellular *B. abortus* A19 in the MFN2-interfered group at 12 h and 24 h, as compared to the control group (siMFN2-Negative group) (P<0.001) *(Fig. 5-C)*. Additionally, at 24 h post-infection, cells were collected and apoptosis was evaluated using flow cytometry. The findings indicated a significantly higher rate of apoptosis in the MFN2-interfered group, as compared to the control group (siMFN2-Negative group) (P<0.001) *(Fig. 5-A,B)*.

Infection of *B. abortus* A19 with Macrophages Overexpressing MFN2 Leads to an Increase in *B. abortus* A19 Intracellular Survival

B. abortus A19 was infected with cells that overexpressed the MFN2 model. The cells were then lysed, and the number of surviving bacteria within the cells was counted. The results showed a significant increase in the number of *B. abortus* A19 within the cells in the MFN2 overexpression group at 24 h, compared to the control group (PCDNA3.1-EGFP) (P=0.020) *(Fig. 6-C)*. Furthermore, at 24 h post-infection, cells were collected and assessed for apoptosis using flow cytometry. The results indicated a significantly lower apoptosis rate in the MFN2 overexpression group, compared to the control group (PCDNA3.1-EGFP) (P<0.001) *(Fig. 6-A,B)*. These results suggest that MFN2 plays a role in down-regulating programmed death in *B. abortus* A19-infected macrophages and supports the intracellular survival of *Brucella*.

Discussion

Brucella is a very "cunning" pathogen that evades the host immune system by translocating to the endoplasmic reticulum in the form of *Brucella* vesicles, leading to chronic infections [21,22]. Macrophages express high levels of MFN2, which not only regulates endoplasmic reticulum stress but also plays a crucial role in immune response regulation [23,24]. MFN2 is also involved in maintaining cellular autophagy. In the absence of MFN2 protein, autophagosomes accumulate, leading to reduced autophagic flux and increased apoptosis. However, this also results in attenuated apoptotic bodies and bacterial phagocytosis [25]. Pathogens have developed various mechanisms to manipulate MFN2 and influence their survival within host cells. In this study, we discovered that MFN2 is responsible for down-regulating endoplasmic reticulum stress and programmed cell death in *B. abortus* A19-infected macrophages, thereby supporting the intracellular survival of *B. abortus* A19.

Macrophages are the main target cells of *Brucella* infections, and in general, *Brucella* undergo immune escape by inhibiting apoptosis to ensure their intracellular survival [26], whereas macrophages themselves enhance the body's killing of pathogenic bacteria and control their intracellular multiplication by regulating apoptosis [27]. Among several apoptotic pathways, the endoplasmic reticulum stress-induced apoptosis pathway is favoured by scholars. The endoplasmic reticulum is involved in the maintenance of cellular homeostasis and can save calcium ions in large quantities, and it is also the main site of *Brucella* proliferation, when pathogenic bacteria infection, calcium ion homeostasis imbalance and redox environment disorders, it will lead to endoplasmic reticulum stress [28], if the endoplasmic reticulum homeostasis can not be restored for a long time, apoptosis will occur, and the ability of *Brucella* to induce cellular endoplasmic reticulum stress has been proved by a large number of scholars [29], the present study found that MFN2 disruption promotes *B. abortus* A19-induced expression of the endoplasmic reticulum stress signature molecule CHOP and GRP78, whereas MFN2 overexpression does the opposite, indicating that deletion of MFN2 enhances the ability of *B. abortus* to induce endoplasmic reticulum stress, which is similar to that found in the mouse fibroblast cell model of MFN2 gene deletion [23], which may be attributed to the fact that MFN2 deletion affected the coupling between the endoplasmic reticulum and mitochondria, disrupting the normal morphology of the endoplasmic reticulum, and possibly because MFN2 deletion interfered with the calcium transfer between the two, resulting in an imbalance of calcium ion homeostasis in the endoplasmic reticulum and aggravating the endoplasmic reticulum stress; in addition, we found that MFN2 interference enhanced the expression of Caspase-3 and BAX, a pro-apoptotic protein induced by *B. abortus* A19, and the flow results also further demonstrated that apoptosis rate increased after MFN2 interference, while the opposite was true for MFN2 overexpression, suggesting that MFN2 deficiency enhances *B. abortus*-induced apoptosis, which is similar to the findings of Lee et al. in *M. tuberculosis*-infected macrophages [30], which may be attributed to the fact that MFN2 deficiency interferes with the normal transmission of calcium ions between the endoplasmic

reticulum and mitochondria, resulting in mitochondrial calcium ions overload and apoptosis, or it may be because MFN2 deficiency exacerbates mitochondrial fragmentation and impairs mitochondrial function and apoptosis occurs, but these are only speculations, and the specific mechanisms remain to be investigated. The results of the intracellular survival assay showed that MFN2 interference decreased the viable bacterial count of *B. abortus* A19 in macrophages, while the opposite was true for MFN2 overexpression, suggesting that the ability of *B. abortus* A19 to survive intracellularly was suppressed to a certain extent after MFN2 deletion, which, combined with the results of the apoptosis assay, suggests that it may be due to the fact that MFN2 deletion exacerbated the cellular apoptosis, so that *Brucella* was deprived of a place to shelter its survival, and thus was recognised and removed by the host, this result is similar to the findings of Lee et al.[30] in *M. tuberculosis*-infected macrophages, and in contrast to the findings of Lobet et al.[31] who found that MFN2 deletion did not affect the survival of *Brucella* in Hela cells, and that the discrepancy the reason may be because RAW264.7 cells are professional phagocytes, which are more sensitive to *Brucella* invasion and have a stronger ability to bind to *Brucella* as well as phagocytose and clear *Brucella* compared to non-professional phagocytes, Hela, or it may be because the *B. abortus* A19 belongs to a weakly virulent strain, which is inherently weaker in terms of surviving in macrophages [32].

In conclusion, as a key regulator of the innate immune response during pathogenic infection, Mfn2 can mediate the down-regulation of endoplasmic reticulum stress and programmed death in *B. abortus* A19-infected macrophages and support the intracellular survival of *Brucella*. The present study provides experimental This study provides an experimental basis for a better understanding of the function of MFN2 gene during *Brucella* infection and the elucidation of the pathogenic mechanism of *Brucella*, as well as a basis for the development of potential targets for preventive and therapeutic programmes against brucellosis.

Declarations

Availability of Data and Materials: Not applicable.

Acknowledgements: Not applicable.

Funding Support: This research was supported by the National Natural Science Foundation of China (32060789, U1803236), and Major Scientific and Technological Projects of Corps (2017AA003).

Conflict of Interest: The authors declare no conflicts of interest.

Declaration of Generative Artificial Intelligence (AI): This article and charts are not written by AI and AI-assisted technology.

Author Contributions: ZY, QY and XD: Conceptualization, Data curation, Investigation, Methodology, Writing the original draft. ZM, CC and YX: Supervision, Resources, Writing, review and editing. All authors read and approved the final manuscript.

References

1. Wang Y, Ma Z, Zhang H, Yi J, Wang Y, LiT, Chen C: The deletion of Omp19 gene of *Brucella abortus* 2308 reduces its survival in mouse macrophageand in mice. *Kafkas Univ Vet Fak Derg*, 26 (6): 749-755, 2020. DOI: 10.9775/kvfd.2020.24280

2. Nandini P, Jakka P, Murugan S, Mazumdar V, Kumar D, Prakash R, Barbuddhe SB, Radhakrishnan G: Immuno-profiling of *Brucella* proteins for developing improved vaccines and DIVA capable serodiagnostic assays for brucellosis. *Front Microbiol*, 14:1253349, 2023. DOI: 10.3389/fmicb.2023.1253349

3. Gomes MTR, Guimarães ES, Marinho FV, Macedo I, Aguiar ERGR, Barber GN, Moraes-Vieira PMM, Alves-Filho JC, Oliveira SC: STING regulates metabolic reprogramming in macrophages via HIF-1αduring *Brucella* infection. *PLoS Pathog*, 17 (5):e1009597, 2021. DOI: 10.1371/journal.ppat.1009597

4. Luizet JB, Raymond J, Lacerda TLS, Barbieux E, Kambarev S, Bonici M, Lembo F, Willemart K, Borg JP, Celli J, Gérard FCA, Muraille E, Gorvel JP, Salcedo SP: The *Brucella* effector BspL targets the ER-associated degradation (ERAD) pathway and delays bacterial egress from infected cells. *Proc Natl Acad Sci U S A*, 118(32):e2105324118, 2021. DOI: 10.1073/pnas.2105324118

5. Muñoz JP, Ivanova S, Sánchez-Wandelmer J, Martínez-Cristóbal P, Noguera E, Sancho A, Díaz-Ramos A, Hernández-Alvarez MI, Sebastián D, Mauvezin C, Palacín M, Zorzano A: Mfn2 modulates the UPR and mitochondrial function via repression of PERK. *EMBO J*, 32 (17): 2348-2361, 2013. DOI: 10.1002/embj.201470050

6. Wang X, Liu Y, Sun J, Gong W, Sun P, Kong X, Yang M, Zhang W: Mitofusin-2 acts as biomarker for predicting poor prognosis in hepatitis B virus related hepatocellular carcinoma. *Infect Agent Cancer*, 13:36, 2018. DOI: 10.1186/s13027-018-0212-7

7. Huang CY, Chiang SF, Lin TY, Chiou SH, Chow KC: HIV-1 Vpr triggers mitochondrial destruction by impairing Mfn2-mediated ER-mitochondria interaction. *PLoS One,* 7 (3):e33657, 2012. DOI: 10.1371/journal.pone.0033657

8. Xu F, Qi H, Li J, Sun L, Gong J, Chen Y, Shen A, Li W: *Mycobacterium tuberculosis* infection up-regulates MFN2 expression to promote NLRP3 inflammasome formation. *J Biol Chem*, 295 (51): 17684-17697, 2020. DOI: 10.1074/jbc.ra120.014077

9. Głowacka P, Żakowska D, Naylor K, Niemcewicz M, Bielawska-Drózd A: *Brucella* - Virulence factors, pathogenesis and treatment. *Pol J Microbiol,* 67 (2): 151-161, 2018. DOI: 10.21307/pjm-2018-029

10. Verbeke, J, Fayt, Y, Martin, L, Yilmaz, O, Sedzicki, J, Reboul, A, Jadot M, Renard P, Dehio C, Renard HF, Letesson JJ, De Bolle X, Arnould T: Host cell egress of *Brucella* abortus requires BNIP3L-mediated mitophagy. *EMBO J*, 42 (14):e112817, 2023. DOI: 10.15252/embj.2022112817

11. Verfaillie T, Garg AD, Agostinis P: Targeting ER stress induced apoptosis and inflammation in cancer. *Cancer Lett*, 332 (2): 249-264, 2013. DOI: 10.1016/j.canlet.2010.07.016

12. Liao, Y, Fung, TS, Huang, M, Fang, SG, Zhong, Y, Liu, DX: Upregulation of CHOP/GADD153 during coronavirus infectious bronchitis virus infection modulates apoptosis by restricting activation of the extracellular signal-regulated kinase pathway. *J Virol*, 87 (14): 8124-8134, 2013. DOI: 10.1128/jvi.00626-13

13. Smith JA, Khan M, Magnani DD, Harms JS, Durward M, Radhakrishnan GK, Liu YP, Splitter GA: Brucella induces an unfolded protein response via TcpB that supports intracellular replication in macrophages. *PLoS Pathog*, 9 (12):e1003785, 2013. DOI: 10.1371/journal.ppat.1003785

14. Bronner DN, O'riordan MXD, He Y: Caspase-2 mediates a *Brucella abortus* RB51-induced hybrid cell death having features of apoptosis and pyroptosis. *Front Cell Infect Microbiol*, 3:83, 2013. DOI: 10.3389/fcimb.2013.00083

15. Fernandez-Prada, C, Zelazowska, E, Nikolich, M, Hadfield, TL, Roop, RM, Robertson, GL, Hoover DL: Interactions between *Brucella melitensis* and human phagocytes: bacterial surface O-Polysaccharide inhibits phagocytosis, bacterial killing, and subsequent host cell apoptosis. *Infect Immun*, 71 (4): 2110-2119, 2003. DOI: 10.1128/iai.71.4.2110-2119.2003

16. Brooks C, Dong Z: Regulation of mitochondrial morphological dynamics during apoptosis by Bcl-2 family proteins: A key in Bak? *Cell Cycle*, 6 (24): 3043-3047, 2007. DOI: 10.4161/cc.6.24.5115

17. Brooks C, Wei Q, Feng L, Dong G, Tao Y, Mei L, Xie ZJ, Dong Z: Bak regulates mitochondrial morphology and pathology during apoptosis by interacting with mitofusins. *Proc Natl Acad Sci U S A*, 104 (28): 11649-11654, 2007. DOI: 10.1073/pnas.0703976104

18. Deng X, Guo J, Sun Z, Liu L, Zhao T, Li J, Tang G, Zhang H, Wang W, Cao S, Zhu D, Tao T, Cao G, Baryshnikov PI, Chen C, Zhao Z, Chen L, Zhang H: *Brucella*-induced downregulation of lncRNA Gm28309 triggers macrophages inflammatory response through the miR-3068-5p/NF-κB pathway. *Front Immunol*, 11:581517, 2020. DOI: 10.3389/fimmu.2021.805275

19. Wang Y, Xi J, Wu P, Zhang H, Deng X, Wang Y, Ma Z, Yi J, Chen C: Small ubiquitin-related modifier 2 affects the intracellular survival of *Brucella abortus* 2308 by regulating activation of the NF-κB pathway. *Innate Immun*, 27 (1): 81-88, 2021. DOI: 10.1177/1753425920972171

20. Zhang H, Wang B, Wu W, Deng X, Shao Z,Yi J, et al: Insights into irr and rirA gene regulation on the virulence of *Brucella melitensis* M5-90. *Can J Microbiol*, 66 (5): 351-358, 2020. DOI: 10.1139/cjm-2019-0393

21. Wang X, Lin P, Li Y, Xiang C, Yin Y, Chen Z, Wang Z, Yang N, Wang Y, Wang Y, Chen C: *Brucella suis* vaccine strain 2 induces endoplasmic reticulum stress that affects intracellular replication in goat trophoblast cells in vitro. *Front Cell Infect Microbiol*, 6:19, 2016. DOI: 10.3389/fcimb.2016.00019

22. Sedzicki J, Tschon T, Low SH, Willemart K, Goldie KN, Letesson JJ, Stahlberg H, Dehio C: 3D correlative electron microscopy reveals continuity of *Brucella*-containing vacuoles with the endoplasmic reticulum. *J Cell Sci*, 131 (4):jcs210799, 2018. DOI: 10.1242/jcs.210799

23. Ngoh GA, Papanicolaou KN, Walsh K: Loss of mitofusin 2 promotes endoplasmic reticulum stress. *J Biol Chem*, 287 (24): 20321-20332, 2012. DOI: 10.1074/jbc.m112.359174

24. Tur J, Pereira-Lopes S, Vico T, Marín EA, Muñoz JP, Hernández-Alvarez M, Cardona PJ, Zorzano A, Lloberas J, Celada A: Mitofusin 2 in macrophages links mitochondrial ROS production, cytokine release, phagocytosis, autophagy, and bactericidal activity. *Cell Rep*, 32 (8):108079, 2020. DOI: 10.1016/j.celrep.2020.108079

25. Sebastián D, Sorianello E, Segalés J, Irazoki,A, Ruiz-Bonilla V, Sala D, Planet E, Berenguer-Llergo A, Muñoz JP, Sánchez-Feutrie M, Plana N, Hernández-Álvarez MI, Serrano AL, Palacín M, Zorzano A: Mfn2 deficiency links age-related sarcopenia and impaired autophagy to activation of an adaptive mitophagy pathway. *EMBO J*, 35 (15): 1677-1693, 2016. DOI: 10.15252/embj.201593084

26. Cui G, Wei P, Zhao Y, Guan Z, Yang L, Sun W, Wang S, Peng Q: *Brucella* infection inhibits macrophages apoptosis via Nedd4-dependent degradation of calpain2. *Vet Microbiol*, 174 (1-2): 195-205, 2014. DOI: 10.1016/j.vetmic.2014.08.033

27. Dong W, Liu D, Li W, Yun L, Qing T, Fang W, Zhang L, Zhang W: The influence of theapoptosis rate and the expression of caspase-3 in the macrophages infected by *Mycobacterium tuberculosis*. *Chin J Immun*, 29 (4): 407-411, 2013. DOI: 10.3969/j.issn.1000-484X.2013.04.017

28. Shin S, Argon Y: Stressed-out endoplasmic reticulum inflames the mitochondria. *Immunity*, 43 (3): 409-411, 2015. DOI: 10.1016/j.immuni.2015.08.027

29. Roop RM 2nd, Barton IS, Hopersberger D, Martin DW: Uncovering the hidden credentials of *Brucella* virulence. *Microbiol Mol Biol Rev*, 85 (1):e00021-19 2021. DOI: 10.1128/mmbr.00021-19

30. Lee J, Choi J, Cho SN, Son SH, Song CH: *Mycobacterium tuberculosis* mitofusin 2-deficiency suppresses survival in macrophages. *Cells*, 8 (11):1355, 2019. DOI: 10.3390/cells8111355

31. Lobet E, Willemart K, Ninane N, Demazy C, Sedzicki J, Lelubre, C, De Bolle X, Renard P, Raes M, Dehio C, Letesson JJ, Arnould T: Mitochondrial fragmentation affects neither the sensitivity to TNFα-induced apoptosis of *Brucella*-infected cells nor the intracellular replication of the bacteria. *Sci Rep*, 8 (1):5173, 2018. DOI: 10.1038/s41598-018-23483-3

32. Cheng Z, Li Z, Yin Y, Lian Z, Abdelgawad HA, Hu H, Guan X, Zuo D, Cai Y, Ding C, Wang S, Li T, Qi J, Tian M, Yu S: Characteristics of *Brucella abortus* vaccine strain A19 reveals its potential mechanism of attenuated virulence. *Vet Microbiol*, 254:109007, 2021. DOI: 10.1016/j.vetmic.2021.109007